

Sensitivity to Cabibbo-Suppressed Λ Production in MicroBooNE

MICROBOONE-NOTE-1112-PUB

The MicroBooNE Collaboration
microboone_info@fnal.gov

May 2022

Abstract

We present a procedure to measure a flux averaged, restricted phase space cross section for direct (Cabibbo suppressed) Λ production using the MicroBooNE detector. This is a rare process, exclusively occurring in anti-neutrino interactions and to maximise the sensitivity of this analysis we combine predictions using the NuMI flux from two data taking periods, one in which this beam was run in neutrino mode and one in anti-neutrino mode. The event selection for this analysis was previously described in MicroBooNE public note 1097 [1]. The calculation of systematic uncertainties is shown and a method to propagate them through to the final cross section calculation is described, with final sensitivities shown in the form of Bayesian posterior distributions on the extracted cross section.

Contents

| | | |
|----------|--|----------|
| 1 | Introduction | 2 |
| 2 | Event Selection | 3 |
| 3 | Systematics | 4 |
| 4 | Cross Section Extraction | 6 |
| 5 | Summary | 7 |
| | Appendices | 8 |
| A | Treatment of Systematic Uncertainties | 8 |

1 Introduction

This note describes the procedure used to estimate the cross section of direct (Cabibbo suppressed, CCQE-like) Λ production in anti-neutrino interactions with argon nuclei in the MicroBooNE detector [2]:

$$\bar{\nu}_\mu + \text{Ar} \rightarrow \mu^+ + \Lambda^0 + X \quad (1)$$

X denotes any additional final state particles with zero strangeness. This is distinct from associated hyperon production, when a K meson or anti-hyperon is produced in addition to the hyperon and there is no change in total strangeness. Direct hyperon production is sensitive to a number of cross section parameters such as axial mass and final state interactions [3].

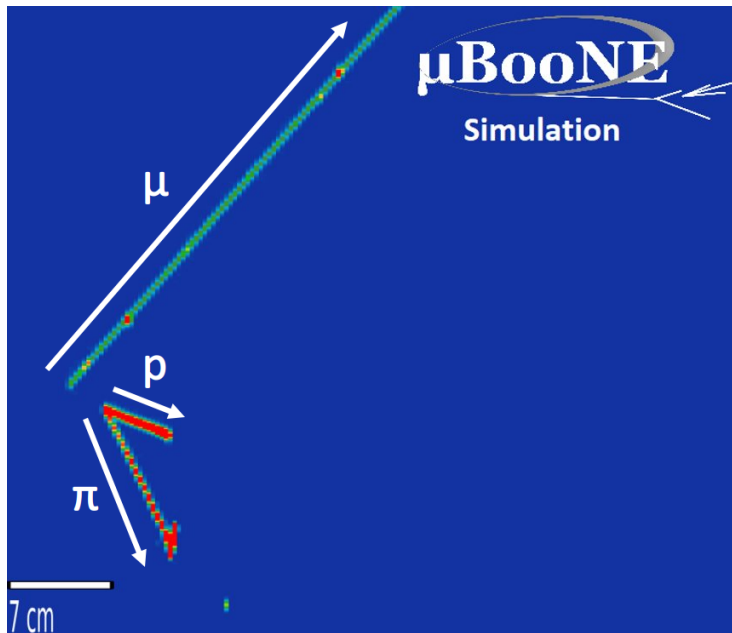


Figure 1: Event display of simulated signal event.

The goal of this analysis is to measure a flux averaged, restricted phase space cross section of this process. We intend to analyse data containing interactions of neutrinos and anti-neutrinos from the neutrinos at the Main Injector (NuMI) beam.

We intend to use a combination of data from running periods: run 1 which was taken during 2015/16 when NuMI beam was run in neutrino mode and run 3, taken in 2017/18 during which the NuMI beam was operated in anti-neutrino mode. These data taking periods correspond to 2.2×10^{20} protons on target (POT) of neutrino mode flux and 4.9×10^{20} POT respectively. We combine predictions from these data taking periods to maximise data and Monte Carlo (MC) simulation statistics. The total flux used is shown in figure 2. We restrict the phase space to only include interactions in which the Λ decays to a $p + \pi^-$, and when the proton and pion have momenta > 300 MeV/ c and 100 MeV/ c respectively.

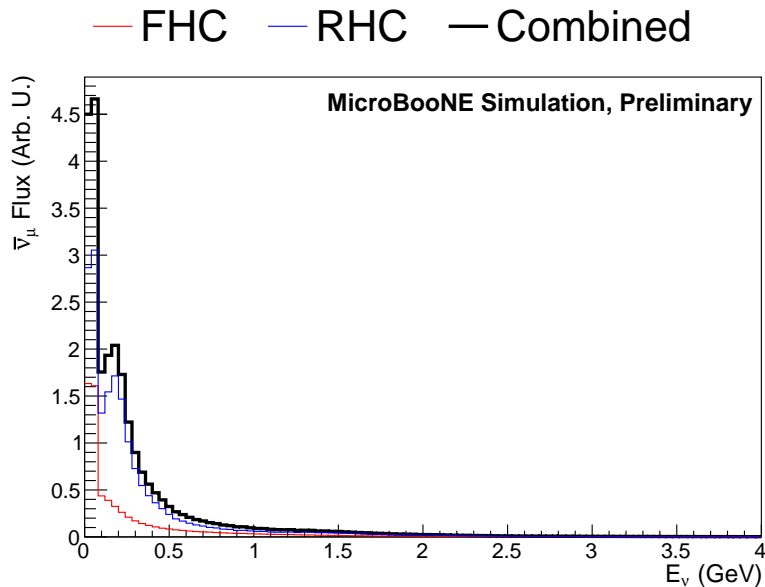


Figure 2: Muon anti-neutrino flux used, corresponding to 2.2×10^{20} protons on target (POT) of neutrino mode flux and 4.9×10^{20} POT of anti-neutrino mode flux.

2 Event Selection

The event selection used is described in detail in MicroBooNE public note 1097 [1], which remains unchanged except a boosted decision tree is no longer used to analyse the kinematics of the Λ candidate¹. A brief overview of the selection is given here.

We employ the Pandora reconstruction framework [4] which identifies a candidate neutrino by isolating the activity believed to be associated with the interaction. Pandora identifies a reconstructed interaction vertex, and classifies the activity corresponding to the neutrino daughter particles into tracks and electromagnetic showers. The selection consists of five stages:

1. A preselection is applied that demands the reconstructed vertex was within the fiducial volume and has at least three associated track like particles and no shower like particles.
2. A muon candidate is chosen by selecting the longest track with a suitable particle identification (PID) score. The PID used is described in [5]. We also demand the muon track starts within 1 cm of the neutrino interaction vertex and has a minimum length of 10 cm for quality.
3. A pair of tracks are selected as a candidate $\Lambda \rightarrow p + \pi^-$ decay. There may be several tracks to choose from and the proton and pion labels must be assigned in the correct order, leading to many possible combinations of tracks. To choose the right pair of tracks, several variables, including particle identification scores and the track/shower classification score produced by Pandora, are fed into an array of boosted decision trees (BDTs). This condenses these variables into a single response value indicating the suitability of that combination of tracks. The pair of tracks with the highest score is used as the Λ decay candidate.
4. The invariant mass (W) and α parameter (defined in [1]) are calculated for the Λ candidate and cuts are placed on these variables to remove background kinematically inconsistent with a Λ decay. We select events with $\alpha < 14^\circ$ and $1.09 < W < 1.14 \text{ GeV}/c^2$. No cut is applied to the track selection BDT response in figure 10 of [1].

¹See section 4 of [1].

5. The connectedness test (described in section 5 of [1]) is used to determine if the proton/pion originate from a true displaced vertex.

The selection achieves an efficiency of 6.8% and purity of 47% when applied to a weighted combination of MC simulations designed to replicate both data taking periods. The numbers of selected events belonging to different categories are shown in figure 3. The selected background is comprised of other events producing Λ baryons, other sources of hyperons (primarily Σ^0 production), events containing neutron-Ar interactions and events with reconstruction defects (labelled as “other ν ” in figure 3).

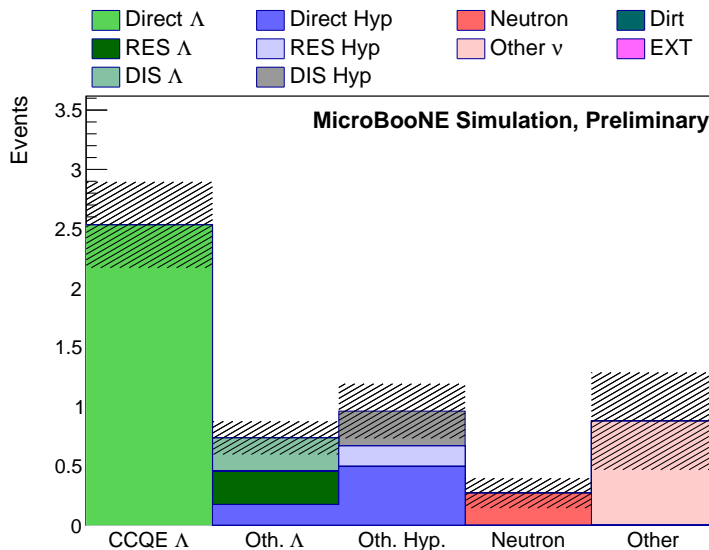


Figure 3: Events passing the selection, broken down by type. Hatched regions indicate the combined MC simulation systematic and statistical uncertainties. Predictions correspond to 2.2×10^{20} POT of neutrino mode flux and 4.9×10^{20} POT of anti-neutrino mode flux.

3 Systematics

Four categories on uncertainty are included:

1. The flux model used: flux uncertainties are divided into two categories, those arising from hadron production modelling and uncertainties related to the beamline geometry. The overall flux uncertainty is relatively low due to the high neutrino energy threshold for Λ production where uncertainties are smaller, with the hadron production being the dominant contribution.
2. Background neutrino interaction cross sections: we use the results of the fits described in [6], with 44 parameters varied in parallel using a multisim technique. Additionally, we use predictions from 7 alternative models to estimate uncertainties resulting from parameters that are difficult to vary continuously.
3. Secondary interactions in the argon outside the daughter nucleus: for reinteraction uncertainties we use the software package Geant4Reweight [7] to propagate the effect of varying proton, charged pion and Λ reinteraction cross sections through the analysis. We assume an uncertainty of 20% on the proton and Λ interaction cross sections, while for the charged pions a pair of multi-target, multi-channel fits were performed using external data to extract uncertainties on the cross sections of individual interaction channels, as described in [7].

To include uncertainties on the neutron interaction cross sections, a fit was performed to data from the CAPTAIN experiment [8], obtaining an uncertainty of 26% on the total n-Ar cross section. This uncertainty is included by re-scaling selected events containing secondary interactions of neutrons by $\pm 26\%$.

4. The detector simulation used: the uncertainties are estimated by simulating a set of neutrino interactions in the MicroBooNE detector, which are fed into several detector models. These sets of events are reconstructed and fed through the selection. The difference between the number of events selected using the default detector model and an alternative model is used as an uncertainty. Four categories of detector uncertainties are considered: Modelling of the quantity of scintillation light produced, the wire response, the space charge effect [9], and the recombination of argon ions.

To propagate uncertainties, we change a parameter/parameters belonging to one of the categories described above, to generate different sets of predictions, called systematic universes. The predicted event rate from both runs is calculated in each systematic universe, before the spread in the event rates of these universes is calculated. This method includes correlations between predictions for the two data taking periods analysed. Systematic uncertainties are included in the cross section extraction procedure by calculating the covariance between the selection efficiency, flux and background event rate.

The largest sources of uncertainty affecting the background are the event generator modelling and the detector simulation. We obtain an overall uncertainty on the expected signal of approximately 14%, with the flux uncertainty dominating over the other categories. The full fractional covariance matrix between the different categories of selected events and fractional uncertainties from different sources are shown in figure 4.

For the signal and first three categories of background, the number of events passing the entire selection is calculated in each systematic universe and used to extract the elements of the fractional covariant matrix. In the case of the “other ν ” background, low MC simulation statistics necessitate an alternative approach where the fractional systematic uncertainty on the events surviving the full selection is approximated with the systematic uncertainty on events surviving the selection without the cuts on α and W . The procedure used is described in appendix A.

This background results from events in which a reconstruction failure created a false secondary vertex. The appearance of these events is not tied to any physics process and the rate these events are produced in the signal region of W and α is correlated with the rate they are generated elsewhere, making this an acceptable approximation.

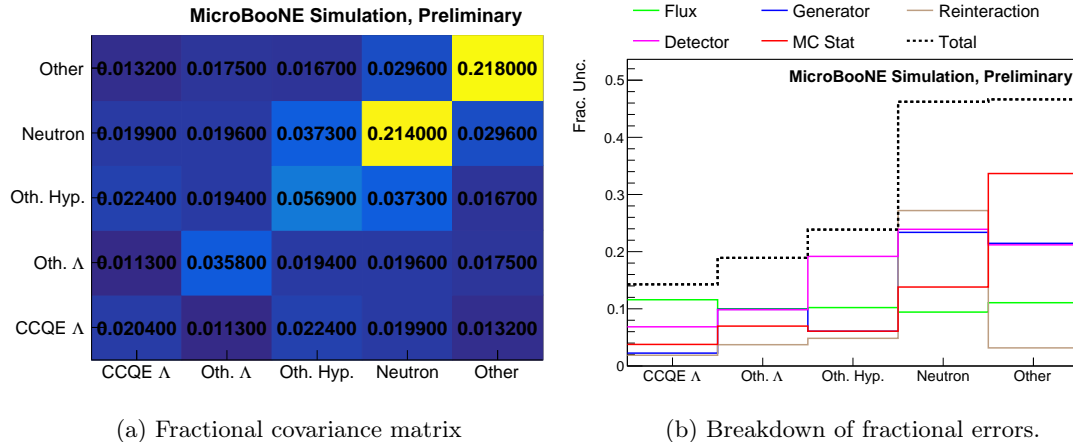


Figure 4: Completed uncertainty calculations, including MC simulation statistical errors.

4 Cross Section Extraction

The restricted phase space cross section σ_* is related to the number of events selected in data N_{Obs} by:

$$\sigma_* = \frac{N_{\text{Obs}} - B}{T\Phi\Gamma\epsilon} \quad (2)$$

where B is the expected number of background events, T the number of Ar nuclei in the fiducial volume, Φ the total anti-neutrino flux, $\Gamma = 0.64$ (the branching fraction for $\Lambda \rightarrow p + \pi^-$ [10]) and ϵ the average selection efficiency. To obtain the equivalent cross section from an event generator/theoretical model, calculate the fraction of Λ 's produced that will decay to a $p + \pi^-$ above the momentum thresholds, f . The reduced phase space cross section is then $\sigma_* = \sigma f/\Gamma$, where σ is the total cross section with no restrictions applied to the final state kinematics.

Monte Carlo simulation and data statistics are non-Gaussian and statistical uncertainties are propagated using a Bayesian procedure, extracting posterior distributions on B and ϵ given the number of events selected in MC simulation samples using the TEfficiency class from Root [11], and the true data event rate N given the number of events observed surviving the selection, N_{Obs} . Uniform priors are used.

We build the posterior distribution of σ_* using a Monte Carlo method: For a fixed value of N_{Obs} , we draw many values of ϵ , B and N from their respective distributions. Systematic uncertainties are included by drawing three smearing parameters, α_ϵ , α_Φ and α_B from a three dimensional Gaussian parameterised by the covariance matrix between ϵ , Φ and B , shown in figure 5. For each set of six parameters, the cross section is calculated:

$$\sigma_* = \frac{N - (B + \alpha_B)}{T(\Phi + \alpha_\Phi)\Gamma(\epsilon + \alpha_\epsilon)} \quad (3)$$

The probability distributions indicate the sensitivity that can be achieved, and are shown in figure 6.

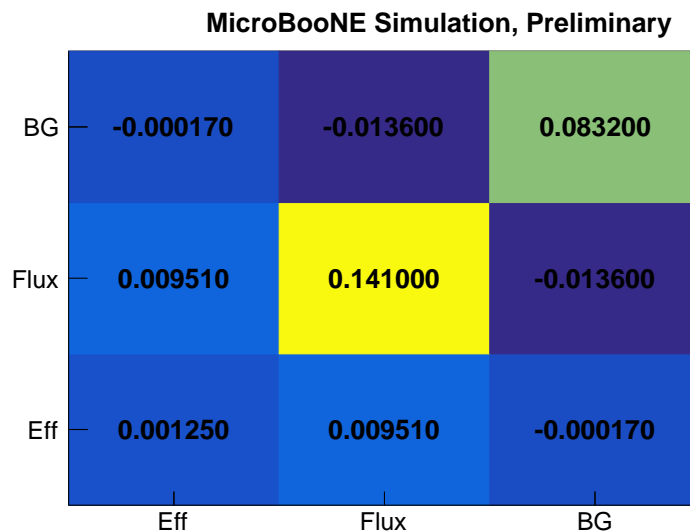


Figure 5: Fractional covariance matrix between the efficiency, flux and expected background.

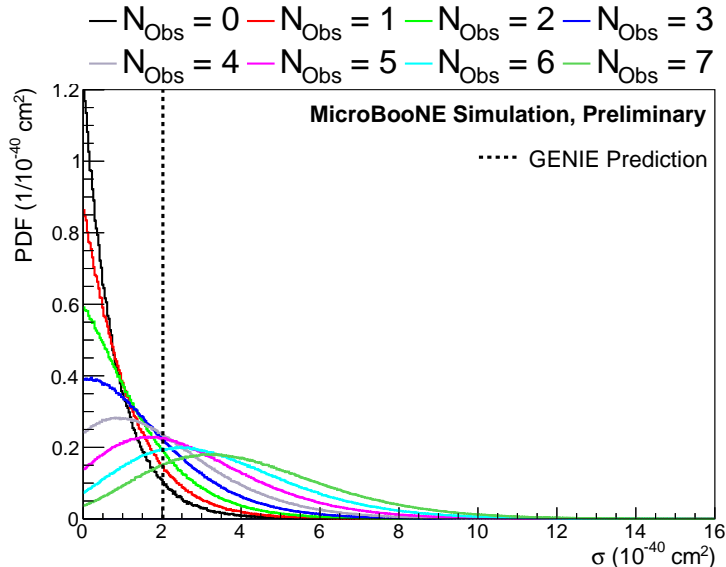


Figure 6: Bayesian posterior PDFs on the extracted cross section given different numbers of data events passing the selection, obtained using equation 3.

5 Summary

The methodology used to estimate the cross section of direct Λ production in the MicroBooNE detector has been described, including the event selection used, calculation of systematic uncertainties, and cross section extraction procedure. We perform calculations of the expected signal and background for a combination of MicroBooNE runs 1 and 3, corresponding to 2.2×10^{20} POT of neutrino mode flux and 4.9×10^{20} POT of anti-neutrino mode flux from the NuMI beam and show the resulting cross sections given different numbers of events surviving the selection, with sensitivities illustrated with Bayesian posterior distributions in figure 6.

References

- [1] MicroBooNE Collaboration. <http://microboone.fnal.gov/wp-content/uploads/MICROBOONE-NOTE-1097-PUB.pdf>. MicroBooNE Public Note 1097.
- [2] R. Acciarri *et al.* (MicroBooNE Collaboration). “Design and Construction of the MicroBooNE Detector”. In: *JINST* **12.02** (2017), P02017.
- [3] C. Thorpe *et al.* “Second class currents, axial mass, and nuclear effects in hyperon production”. In: *Phys. Rev. C* **104.3** (2021), p. 035502.
- [4] R. Acciarri *et al.* (MicroBooNE Collaboration). “The Pandora multi-algorithm approach to automated pattern recognition of cosmic-ray muon and neutrino events in the MicroBooNE detector”. In: *Eur. Phys. J. C* **78.1** (2018), p. 82.
- [5] P. Abratenko *et al.* (MicroBooNE Collaboration). “Calorimetric classification of track-like signatures in liquid argon TPCs using MicroBooNE data”. In: *JHEP* **12** (2021), p. 153.
- [6] P. Abratenko *et al.* (MicroBooNE Collaboration). “New $CC0\pi$ GENIE model tune for MicroBooNE”. In: *Phys. Rev. D* **105.7** (2022), p. 072001.
- [7] J. Calcutt *et al.* “Geant4Reweight: a framework for evaluating and propagating hadronic interaction uncertainties in Geant4”. In: *JINST* **16.08** (2021), P08042.

- [8] B. Bhandari *et al.* (CAPTAIN Collaboration). “First Measurement of the Total Neutron Cross Section on Argon Between 100 and 800 MeV”. In: *Phys. Rev. Lett.* **123.4** (2019), p. 042502.
- [9] P. Abratenko *et al.* (MicroBooNE Collaboration). “Measurement of space charge effects in the MicroBooNE LArTPC using cosmic muons”. In: *JINST* **15.12** (2020), P12037.
- [10] P. A. Zyla *et al.* (Particle Data Group). “Review of Particle Physics”. In: *PTEP* **2020.8** (2020), p. 083C01.
- [11] <https://root.cern.ch/doc/master/classTEfficiency.html>. Accessed April 2022. Root version 6.16 used.

Appendices

A Treatment of Systematic Uncertainties

The procedure for estimating the uncertainty on the “other” category of background is described here. Let X be the number of events belonging to one of the other four categories of events (CCQE Λ , Other Λ etc.) passing the entire selection. Let Y_{Full} be the number of “other” events passing the entire selection, and Y_{NoCuts} be the number of “other” events passing the selection without applying the cuts on α and W .

We calculate the fractional covariance between X and Y_{NoCuts} :

$$\text{FCov}(X, Y_{\text{NoCuts}}) = \frac{\text{Cov}(X, Y_{\text{NoCuts}})}{XY_{\text{NoCuts}}} \quad (4)$$

The covariance between X and Y_{Full} is approximated with:

$$\text{Cov}(X, Y_{\text{Full}}) \approx \text{FCov}(X, Y_{\text{NoCuts}})XY_{\text{Full}} \quad (5)$$

The calculation of the squared uncertainty in Y_{Full} , $\text{Cov}(Y_{\text{Full}}, Y_{\text{Full}})$ is:

$$\text{FCov}(Y_{\text{NoCuts}}, Y_{\text{NoCuts}}) = \frac{\text{Cov}(Y_{\text{NoCuts}}, Y_{\text{NoCuts}})}{Y_{\text{NoCuts}}^2} \quad (6)$$

$$\text{Cov}(Y_{\text{Full}}, Y_{\text{Full}}) \approx \text{FCov}(Y_{\text{NoCuts}}, Y_{\text{NoCuts}})Y_{\text{Full}}^2 \quad (7)$$